Effect of nozzle geometry on the mixing of single and multiple jets

Gamal H. Moustafa and A.M. Alam El-Din
Department of Mechanical Power Engineering, Faculty of Engineering, Menoufia University, Shebin El-Kom, Egypt.

An experimental investigation has been conducted of the interaction and mixing of twin and triple subsonic and supersonic jets issuing from parallel circular, triangular and elliptic nozzles of equal exit area issuing into an ambient still air. The aim is to study the effect of nozzle geometry on the jet interaction to achieve good mixing. Different nozzle geometries, circular, triangular and elliptic were used to produce the jets. For multiple jets, the spacing between the nozzle axes was kept constant (s/d_e = 3.5). Measurements were made for the range of stagnation pressure from 1.3 to 2.5 atmospheres. The flow field of the single jet was found to be characterized by the presence of three distinct regions, defined by the axial mean velocity decay, which are referred to as: a potential core region, a two dimensional type region, depends on the nozzle geometry, and an axi-symmetric type region. In the case of twin and triple jets, there are three regions, which could also define the flow field: the converging, merging and combined regions. The half width of the single jets varies linearly with downstream distance, with different slopes for different nozzle geometry. The spread rate of twin and triple jets is negligible in the near field (x/d_e < 10) while, in the far field, such jets follow the single jet with higher spreading rates. The elliptic and triangular jets were found to be capable of entraining large amounts of surrounding fluid relative to that entrained by the circular jet for subsonic and supersonic flow regimes, indicating good mixing. The flow pattern obtained by the oil film visualization gives details of the spreading and interaction of multiple jets. There are good agreement between measurement and visualized results.

يتناول البحث دراسة تأثير شكل البوق على أداء النفث وعملية الخلط المصاحبة له وذلك عند ظروف ابتدائية تبدأ من 1.3 حتى 2.5 ضغط جوى وبذلك تم تصميم أبواق ذات أشكال دائرية ومثلثة و بيضاوية المقطع بحيث كان مساحة المقطع عند المخرج متساوية كى تسهل عملية المقارنة بينها. وكان الهدف أيضا من الدراسة هو توضيح تأثير شكل الأبواق على عملية الاتحاد والخلط في حالة استخدام أكثر من نفث. وبينت التجارب أن مجال النفث المفرد يتكون من ثلاث مناطق رئيسية تحدد ملامح النفث هى منطقة مركزية وهى منطقة قلب النفث ومنطقة ثنائية الأبعاد تعتمد أساسا على شكل مقطع البوق وأيضا منطقة دائرية الشكل وهى ذات ملامح واحدة في جميع الحالات بغض النظر عن شكل مقطع البوق حيث يتحول النفث المثلث والبيضاوى إلى النفث الدائري في المنطقة البعيدة من مخرج البوق. وفى حالة استخدام أكثر من بوق فقد وجد أن هناك ثلاث مناطق تحدد الشكل العام للأداء وهى منطقة التقارب وأخرى هي منطقة التداخل وأخرى بعيدة عن مخرج البوق هي منطقة الاتحاد مثلها مثل في حالة النفث الغير قابل للانضغاط ولا تعتمد على شكل مقطع البوق. ووجد أن النفث المفرد ينتشر انتشارا خطيا في جميع الحالات وان النفث البيضاوى انتشاره أكبر من كلا من النفث المثلث والدائري صاحبا كمية أكبر من الوسط المحيط معطيا أكبر معدل إخماد مما يجعل عملية الخلط احسن ويرفع من الأداء وكذلك الاتحاد والاندماج في حالة النفث المتعدد وبينت التجارب عند تصوير مجال النفث أن هناك اتفاق مع النتائج المقاسة.

Keyword: Triangular, Elliptic jets, Triple jets, Jet mixing, Flow visualization.

1. Introduction

Extensive experimental studies in high-speed jets by Schadow et al. [1], Gutmark et al. [2] and earlier by Ho and Gutmark [3] have revealed considerable reduction in the jet growth rate with an increase in compressibility. The use of nonconventional nozzle geometry, such as rectangular, triangular and elliptic is the way to avoid this problem and also to achieve enhanced mixing. As noted by previous researchers (Schadow et al. [4]), based on the coherent structure dynamics in subsonic shear layers, methods have been developed to actively and passively control the flow field evolution, and subsequently the mixing process. For passive control, the unique shear flow development of noncircular nozzles with elliptic, rectangular, and other nonconventional cross section geometry were used to improve performance of various types of subsonic ramjets. The fact is

© Faculty of Engineering, Alexandria University, Egypt.

noncircular jets usually spread faster than circular jets.

Noncircular jets issuing from noncircular nozzles are used in many engineering applications such as the aerospace, combustion chamber of jet engines, boiler furnaces, and gas turbine plants of electric power utilities. In fact, such jets have shown to be capable of entraining large amounts of surrounding fluid relative to that entrained by a circular jet, Koshigoe, et al. [5]. The Large amount of entrainment induced rapid mixing which is required for good performance in most applications. This feature is associated with self induction of the elliptic coherent structures in an elliptic jet, which results in a large spreading rate in the minor axis plane relative to that in the major axis plane producing axis switching.

Also, flow measurements for a jet from a triangular nozzle show that the spreading rate of the flow at the flat sides is large than at the vertices, producing a switch in the shape orientation in the downstream from the nozzle exit, Schadow et al. [6]. Quinn [7] provided that the inversion of the jet shape occurs at about five equivalent diameters (D_e) downstream from the slot exit plane. For the case of an elliptic free jet, Quinn [8] showed also that there are two switches of the major and minor axes and the jet attains an axisymmetric shape at about 30 equivalent slot diameters from the exit plane.

In fact, noncircular jets have been the topic of extensive research in the last fifteen years, for the field of combustion. These jets were identified as an efficient technique of passive flow control that allows significant improvements of performance in various practical systems. Gutmark and Grinstein [9] reported that the applications of noncircular jets include improved large-and small-scale mixing in low-and high-speed flows, and enhanced combustor performance, by improving combustion efficiency, reducing combustion instabilities and undesired emissions.

Also, it is well known that mixing enhancement in compressible free shear layer flows with high connective Mach numbers is difficult. One design strategy to get good mixing is to use multiple nozzles. The multiple jets, issued parallel from a number of nozzles, interfere with each other. The interactions of twin round free jets have been studied for a long time, Okamoto et.al. [10]. The rectangular jets have been investigated by many, Tanaka [11, 12] and Krothapalli et al. [13]. Tanaka and Nakata [14] have examined the interference of two-dimensional parallel triple jets. The flow parameters influenced the flow field of such jets are initial flow conditions, spacing between jets, angle between jet axes, nozzle geometry, the end wall, surrounding field etc., Miller and Comings [15]. In the triple jet, the two outer jets set up a twin jet flow with an associated reverse flow between them. When the central jet is introduced in the reversed region, it has to overcome the reversed flow. Therefore, the flow field of the triple jet is largely affected by the behavior of the central jet. In the case of non-circular jets, the axis switching as well as the flow orientation in the down stream significantly affect the flow pattern of such mixed jets.

In fact, no work so far is available explains the interaction of multi free jets issuing from triangular and elliptic nozzles. Also, most of previous work on triangular and elliptic jets has focussed on incompressible turbulent flows. Thus, no available work that examines the flow of a high-speed free jet issuing from triangular and elliptic nozzles, which is the aim of the present study. Therefore, the present investigation gives information for the flow of high-speed triangular and elliptic free jets for the range of stagnation pressure from 1.3 to 2.5 atmospheres. Also, the interaction and mixing processes of twin and triple jets issuing from such nozzles are also studied. The flow pattern is visualized using an oil film technique.

2. Experimental set-up and procedure

A high-pressure blow down air supply system was used to produce the jet. Fig. 1. shows the schematic diagram of the experimental set-up and test section. Two air compressors (37 kw each) with a discharge of 0.1 kg/sec were used to supply air, which was restored in air tank (1.6m x 2.5 m^2). The pressure in air tank was automatically controlled, at a maximum value of 8 bar. The

air before restore was passed through an air dryer and oil separator. Then, the air was passed through a 3`` diameter pipeline to a settling chamber. The pipeline control section includes a gate valve followed by a pressure-regulating valve. Two mesh wire screens were fixed in the settling chamber to reduce air disturbances before discharged through nozzles into the atmosphere. Circular, equilateral triangular and elliptic nozzles of equal geometric area were fabricated of Aluminum and were polished to make surfaces as smooth as possible. The exit diameter (d_e) of the circular nozzle is 10 mm. The triangular and elliptic nozzles were designed to give an equivalent diameter (D_e) of 10 mm, Fig.2. This is to keep the equivalent exit area of the nozzle be constant. In the case of twin and triple jets, a connecting end wall was placed between nozzles so that the jets issue from one standing plate and the entrainment between the converging jets was restricted, Fig.2.

Measurements of total and static pressures were made along the y and z directions for different downstream locations in the x direction, Fig.2. A static probe and a Pitot tube probe of 0.5 mm inner diameter and 1 mm outer diameter were used to measure the static and total pressures. The probes were fixed on a 3 dimensional traverse system, which has a pitch of 1 mm in all directions. Experiments were made, at first, on the single jet and then the procedure was repeated for multijets. Water and mercury U-tube manometers were connected to the pressure probes that can help for pressure reading which was uniform within ± 0.2 %. The uncertainty in the probe measuring location was ± 0.15 %. For the case of multi-jets, all nozzles were made on the same standing with their axes parallel each other. The distance between nozzle axes was kept constant at 35 mm with uncertainty of ± 0.1 %.

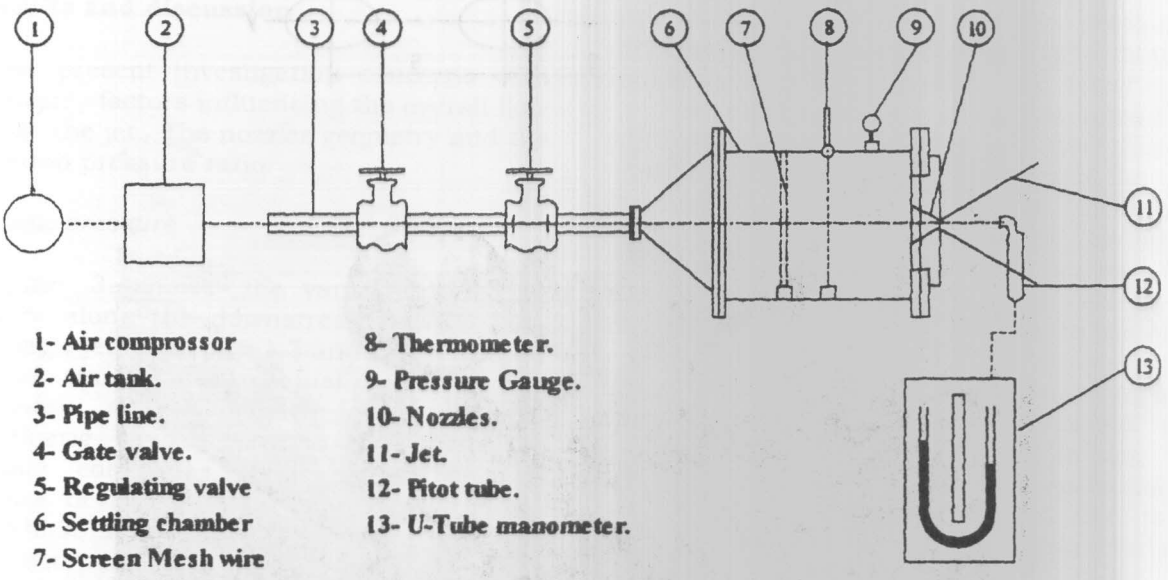

Fig. 1. Experimental set up and test section.

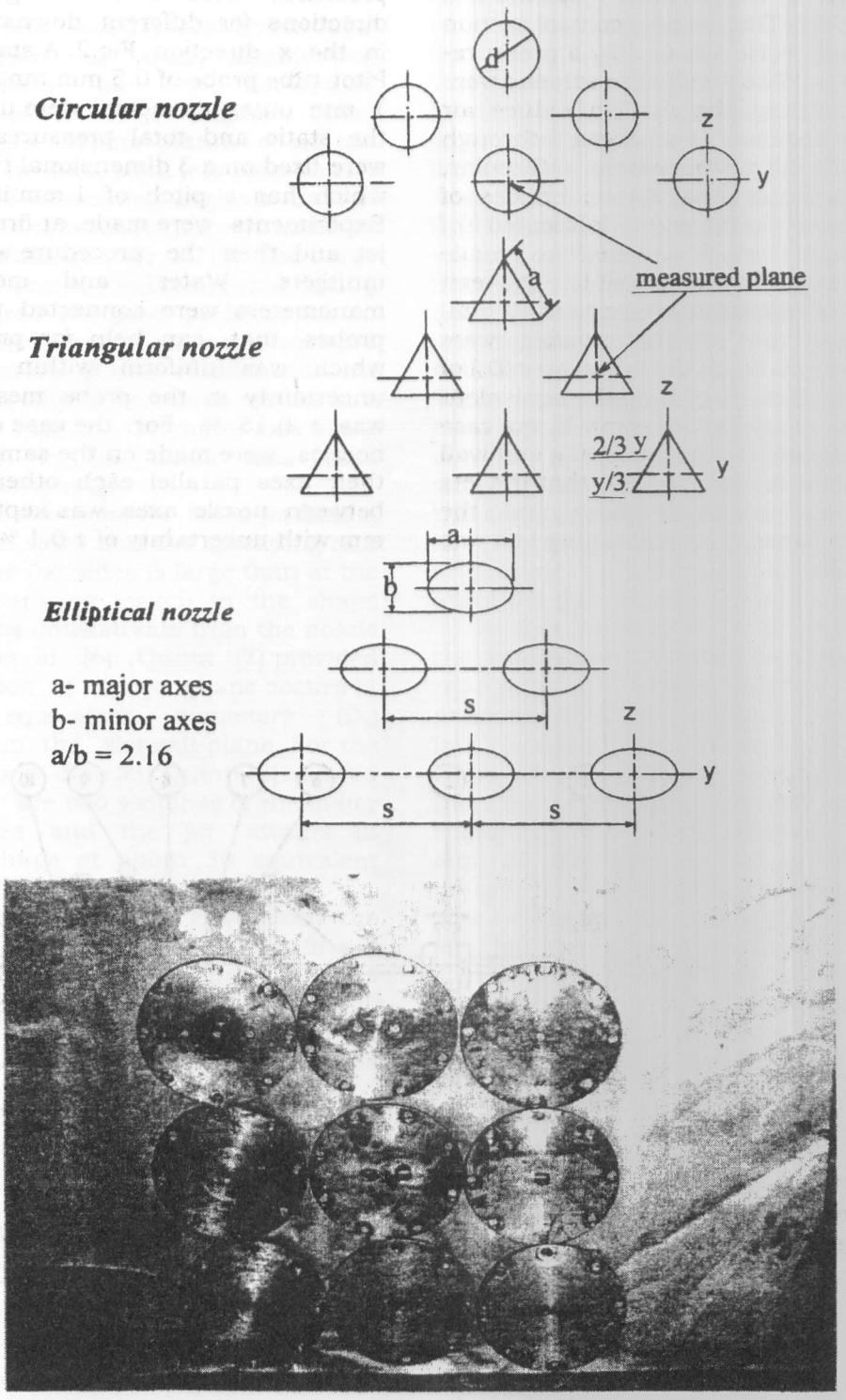

Fig. 2. Nozzles geometry.

The stagnation pressure was measured using a digital manometer, which varied from 1.3 to 2.5 atmospheres with uncertainty of ± 0.1%. The nearest building walls were kept sufficiently far from the tunnel to exclude their effects. The stagnation temperature was measured using a digital thermometer whereas; a mercury thermometer was used to measure the ambient temperature. The temperature reading was uniform within ± 0.28%. The ambient atmospheric pressure was measured using a barometer within ± 0.25%. An oil film technique was used to visualize the flow pattern to detect the effect of nozzle geometry on the jet spreading, mixing and interaction processes. The oil was spread on a plate, which was set horizontally at 1 cm from the lower edge of the nozzle, for all nozzles geometry. The jet was allowed to issue. Hence, the soft nondrying oil used in experiments would flow along the painted surface and trace out the flow pattern. Then, the jet was allowed to grow up for few seconds before the photographs were taken. The oil film was covered a distance from the nozzle exit in the a-direction, around to 200 d_e . The process was repeated and photographs wee taken for single, twin and triple jets.

3. Results and discussion

The present investigation concerns with two major factors influencing the overall flow field of the jet. The nozzles geometry and the stagnation pressure ratio.

3.1 Static pressure

Figure 3 shows the variation of static pressure along the downstream distance for the single jet at p_o/p_a = 1.3 and 2.5. It is seen that the static pressure, just downstream of the nozzle exit is slightly lower than the atmospheric pressure when the jet is at subsonic conditions. This is due to the existence of the common end wall between the jets, which restrict the ambient entrainment. Far downstream (x/d_e = 8) from the nozzle exit plane, the static pressure equals the ambient pressure. When the jet be within the supersonic flow regime (the under-expanded sonic jet), the static pressure, in the near region shows variation under and above the atmospheric pressure. The reason is due to the existence of shock waves within the jet. The position of these shocks is varied as the jet issued from different nozzles geometry. This result indicates that the jet structures in the inner region just downstream of the nozzle exit plane are strongly affected by nozzles geometry, circular, triangular or elliptic. Therefore, the initial development is different of such jets, which affects the jet behavior, spreading and decay rates.

3.2 Total pressure

Figure 4 shows the total pressure distributions along the y-direction of the single jet issuing from circular, triangular and elliptic nozzles, for different stagnation pressure ratios (p_o/p_a = 1.3 and 2.5). The corresponding Mach numbers are (M_e=0.63 and 1.23) respectively, (see gas dynamic tables, Shapiro, [21]). It is seen that the stagnation pressure ratio as well as the nozzles geometry affects the variation of the total pressure. The maximum total pressure is different as the nozzles geometry is changed, indicating different spreading and decay rates.

The elliptic and triangular jets spread (the width in the y-direction) much faster than the circular jets. The axis switching is the main mechanism behind the enhanced entrainment properties of non-circular jets relative to comparable circular jets. The axis switching results with a large spreading rate in the minor axis plane relative to that in the major axis plane. The elliptic jet shows much spreading rate than other jets, indicating more surrounding entrainment associated with such a jet, implying improved mixing. The reason is related to the self-induction of vortices that are being distorted due to the variation of their instability characteristics around their circumference.

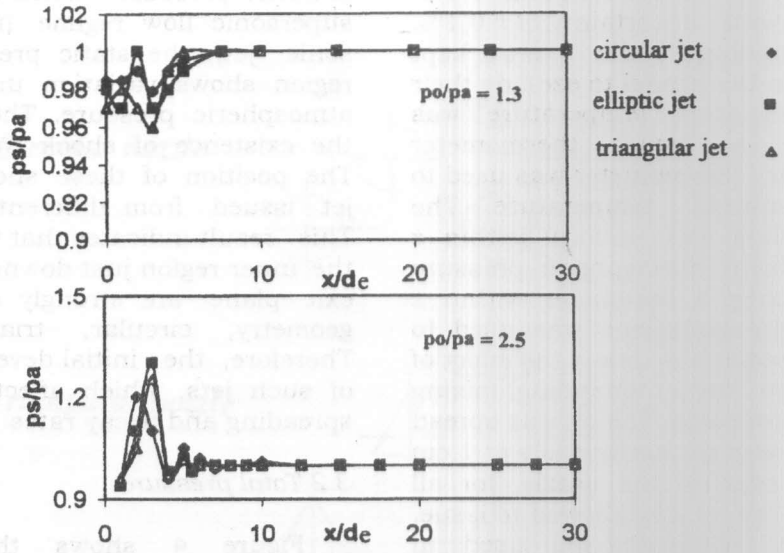

Fig. 3. Variation of static pressures of single jet.

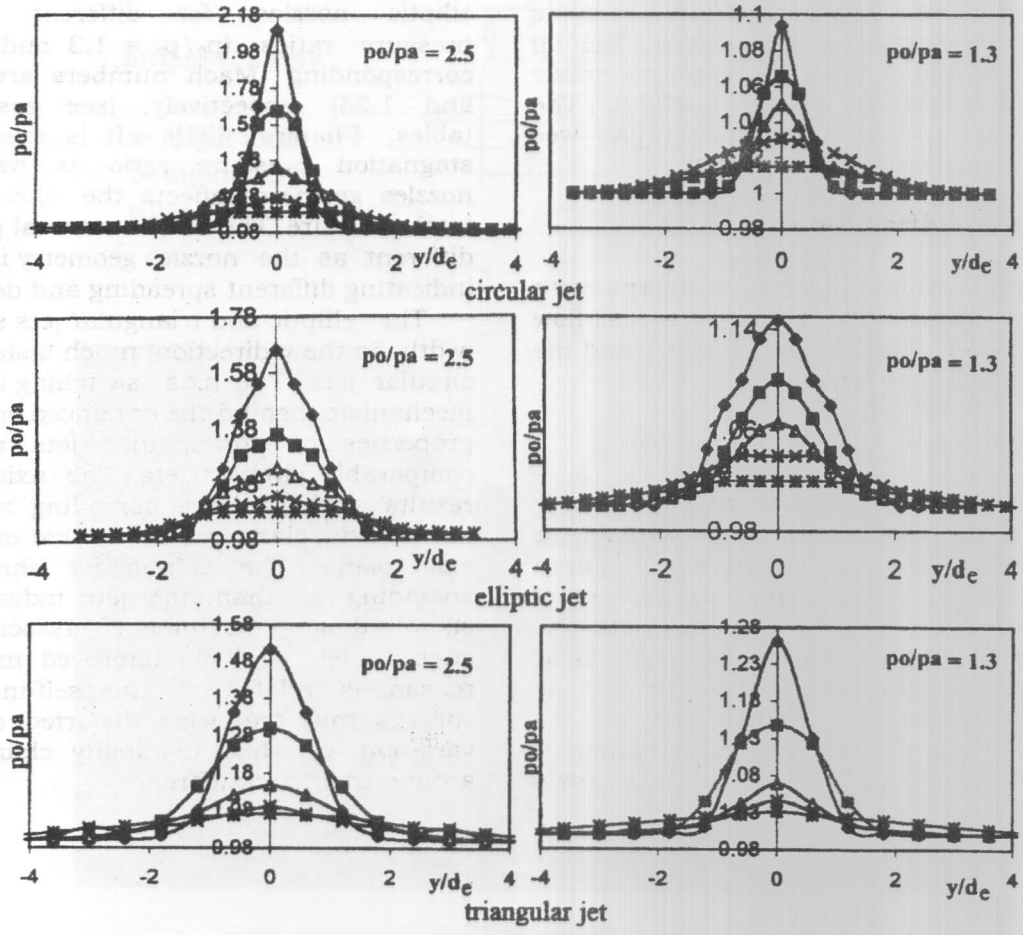

Fig. 4. Distributions of total pressure for single jet.

The spreading of supersonic triangular and elliptic jets is larger than that of subsonic jets. The increase of spreading rate of elliptic and triangular supersonic jets is related to the series of bouncing expansion and compression waves that generate a non-symmetric structure of cells (Schadow, et. al. [4]). In fact, the coexistence of large-scale structures at the flat sides of the triangular jet and small scale eddies at the vertices make the triangular jet an attractive flow configuration for combustion systems. In the case of an elliptic jet, the flow field development is characterized by the dynamics of large scale vortex rings and hairpin (braid) vortices, and by strong vortex interactions leading to a more disorganized flow regime characterized by smaller-scale elongated vortex tubes. Also, finally seen are both triangular and elliptic jets attaining an axisymmetric shape at about 30 equivalent diameters (30 D_e) downstream of the nozzle exit plane.

Figure 5 shows the distributions of total pressure along the y-direction for the twin jet. The maximum total pressure of the jet and its location from the y-axis decreases with an increase of the distance from the nozzle exit plane. Due to the common wall and air surrounding flow entrainment there is a sub-atmospheric region between the two jets, leads to an attraction between the jets. Therefore, the two jets attract each other, mix and finally combine to appear as a single jet. The merging and combined locations with the x-direction depend upon the stagnation pressure ratio and nozzles geometry. In general, the merging point locates at $5 < x/d_e < 15$ and the combined point locates at $20 < x/d_e < 30$. The maximum total pressure becomes at the symmetry axis between the two jets for $x/d_e > 30$ and decays as the single jet. The jet width increases with the distance from the nozzle. The amounts of entrainment and jet width depend upon the flow regime (subsonic or supersonic) and the nozzles geometry.

In fact, the main feature of the twin jet is the appearance of a sub-atmospheric region between the jets, owing to the entrainment of the surrounding fluid and the end wall effect. Thus, the two jets attract each other due to the deflection of their axes and finally join together. The spreading of the twin jet is much larger than that of the single jet and its value depends upon the type of jets (circular, triangular or elliptic). The non-circular jets (triangular and elliptic) show much spreading rate than those of the circular jets, as also given for the case of the single jet. The main reason can be explained as follows: Experiments revealed complex vortex evolution and interaction related to self induction of the asymmetric coherent structures and interaction between azimuthal and axial vortices, which lead to axis switching in the mean flow field. Such a phenomenon is the reason for the large spreading rate associated with non-circular jets, Ho and Gutmark [3].

The distributions of total pressure at different axial locations are given in Fig.6 for circular, triangular and elliptic triple jets. The strength of the central jet is equal to that of the outer jets. It is known that the two outside jets set up a dual jet flow with an associated reverse flow. The central jet overcomes such a flow in which the central jet discharges opposite to the reversed flow induced by the outside jets. There a significant region exists where the mean flow profile of the individual jets behaves quite independently of each other. However, measurements show a sub-atmospheric pressure region between the jets near the nozzle exit. Also, it is observed that, with the merging of total pressure profiles, there is an interaction between the profiles, with the peak total pressure of the outer jets shifting toward the central axis. At about $x/d_e = 15$, the three jets have merged together to form a single jet. Improved mixing in the case of multiple jet results in a rapid decrease in the peak total pressures. At about $x/d_e = 30$, the differences between the triple and single jets are not noticeable, ether

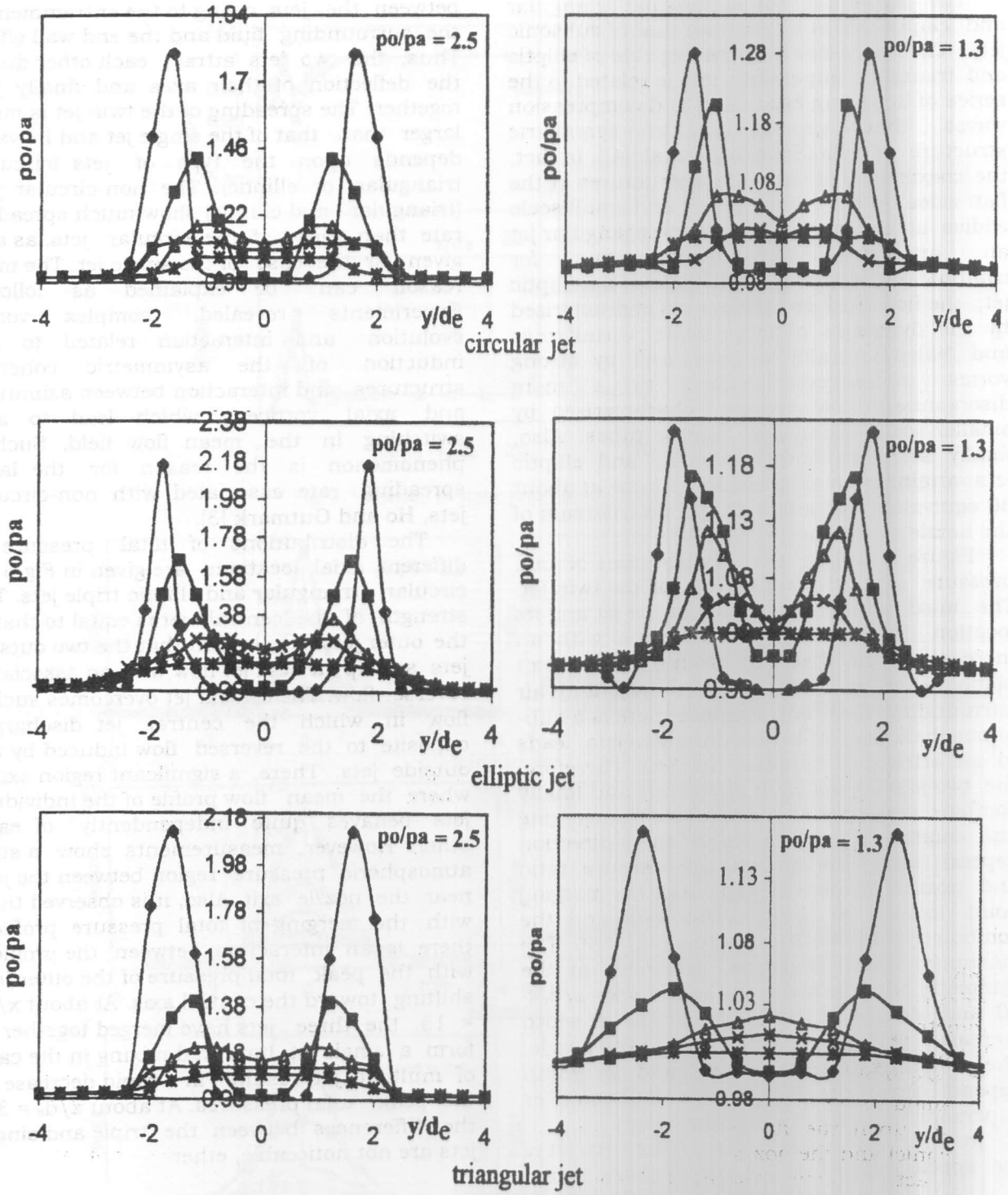

Fig. 5.Distributions of total pressure for twin jet

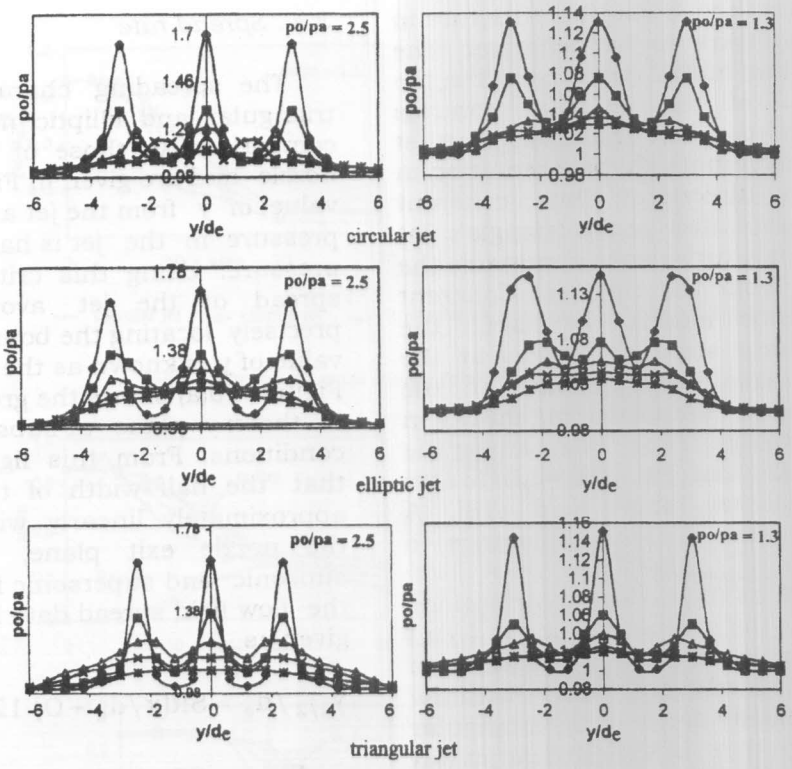

Fig. 6 Distributions of total pressure for triple jet.

in terms of total pressures or the extent of spreading rate. As in the case of incompressible jets, three regions define the flow field: converging region that begins at the nozzle exit plane and extends to the point where the jets start to merge. The merging region, that begins downstream of the merging point and continues to the section where the streamwise velocity in the central plane is maximum. The combined region, that begins after the jet merged, where the jets combine to resemble a single jet flow, Lin and Sheu [16].

3.3 Velocity decay

The decay of mean velocity of the single jet issuing from circular, triangular and elliptic nozzles is shown in Fig.7. The mean velocity was calculated from the measured total pressure within the jet using the one dimensional isentropic flow relations. The trend of the velocity decay for all cases is similar. Thus, as for the case of incompressible jets, the flow field is characterized by the presence of three distinct regions. These regions are potential core region, a two dimensional-type region or the transition region that depends on the nozzles geometry and an axisymmetric type region. The decay rate changes with the nozzles geometry. The length of the potential core is about 5 d_e for the circular jet while that is less than 5 d_e for the triangular and elliptic jets, indicating faster decaying, which resulting a good mixing. The faster decaying associated with triangular and elliptic jets is due to the axis-switching phenomenon. Koshigoe, et. al. [17] provided that the initial development of axis switching for elliptic jets is characterized by the deformation of the coherent structures in the jet. The deformation of the structure and subsequent development of axis switching can be associated with the self-induction of the asymmetrical distribution of the vorticity in the jet, which causes differences in roll-up locations. The portions of the elliptic vortical structure around the major axis roll up slightly farther downstream than those of the

minor axis. Thus, the rolled-up structure in elliptic shape appears to be deformed. The deformation is the initial development in the axis switching of the jet that controls entrainment into the jet. The triangular jet undergoes a switch in its shape orientation in the downstream direction. Thus, coherent structures are generated at the triangle's flat side, but fine-scale turbulence dominates the flow emanating from the vertices. Coherent structures enhance mixing. In fact, the coexistence of large-scale structures at the flat-sides and small-scale eddies at the vertices is necessary for enhancing mixing in the chemical reaction. For comparison the curve for a rectangular jet (M_e =1.5) is also shown, Raghunathan and Reid [18]. A rectangular jet takes a longer distance to decay.

The velocity decay (u_j/u_o) and distributions of velocity along the symmetric axis (u_{ax}/u_o) for the twin jet is given in Fig.8. The maximum velocity decay is clearly noticeable with the elliptic jet. The velocity decay of the triangular jet is larger than that of the circular jet but less than that of the elliptic jet. The decay of the twin jet is more than that of the single jet indicating more surrounding flow entrianment. The velocity at the symmetric axis increases from a negative value and reaches maximum at some location in the x direction. Then, it decreases following the same trend of the single jet, for all cases. Also, seen is the two jets join together at $10 < x/d_e < 15$.

A plot of (u_j/u_o) vs. x/d_e is shown in Fig.9 to indicate the decay of the axial mean velocity of triple jets. The decay increases in the case of multiple jets than that for the case of the single jet. Significant decay occurs between x/d_e = 5 and 20 for the single jet. The corresponding values for the triple jet are x/d_e = 4 and 15.

3.4 . Spread rate

The spreading characteristics of jets from triangular and elliptic nozzles are studied in comparison to those of a jet from a circular nozzle and are given in Fig.10. Here $y_{1/2}$ is the value of y from the jet axis at which the total pressure in the jet is half the centerline total pressure. Using this criterion to express the spread of the jet avoids the difficulty in precisely locating the boundary of the jet. This value of y is known as the half width of the jet. Figure 10(a) shows the growth of the single jet in the x-y plane at subsonic and supersonic conditions. From this figure, it can be seen that the half width of the single jet grows approximately linearly with the distance from the nozzle exit plane, for both cases of subsonic and supersonic flow regimes. Hence, the flow field spread data have been fitted and given as

$$y_{1/2}/d_e = SR(x/d_e + O) \quad 12 \le x/d_e \le 30 .$$

Where SR is the spreading rate (the value of the jet width in the y direction at the corresponding location in the x direction) and O is the geometric virtual origin. The values of SR and O change with the type of jet, circular, triangular and elliptic and also with the initial flow condition (subsonic and supersonic). Also, for the case of noncircular jets the values of SR and O change from x-y plane to x-z plane. These results agree well with those of Namer and Otugen, [19] and Quinn [8]. The values of SR and O in the x-y plane are given in the following table:

	Subsonic		Supersonic	
	SR	O	SR	O
Elliptic jet	0.092	-5.85	0.087	-5.9
Triangular jet	0.068	-6	0.0729	-6.2
Circular jet	0.096	-13.53	1.127	-13.89

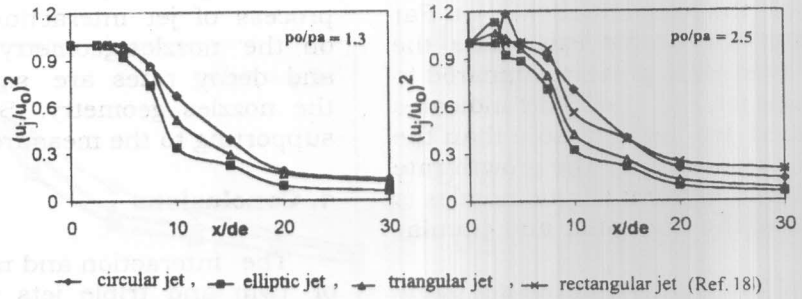

Fig . 7. Decay of axial mean velocity for single jet

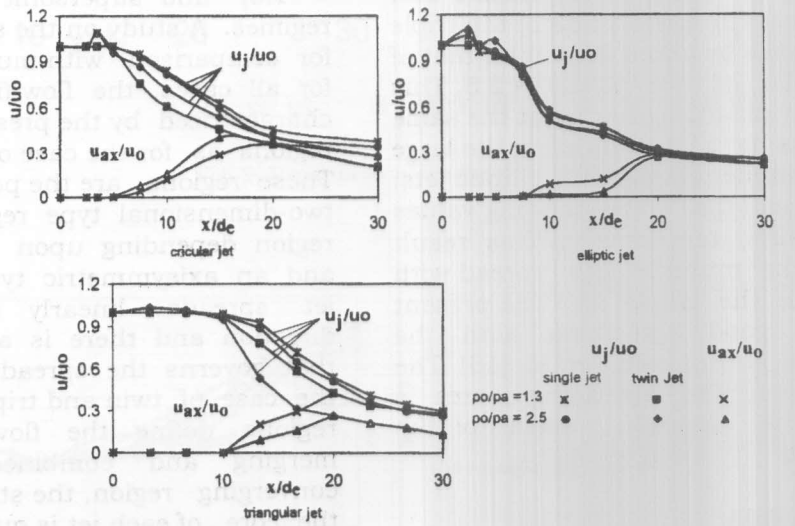

Fig. 8. Decay and distributions of axial mean velocity for twin jet.

These values for the case of the elliptic jet tested by Quinn [8] are SR =0.127 and O=-5.852 for the range of $12< x/d_e <37.5$, at the nozzle exit velocity = 60 m/sec (Re = 2.08 x 10^5). For the case of a rectangular jet tested by Namer and Otugen [19] these values are SR = 0.095 and O = -6, for the range of $12 < x/D < 120$, for the nozzle exit velocity ranged from 5.1 to 35.6 m/sec (Re =1000 to 6000). Here, D is the nozzle width.

The half width of the circular jet at the subsonic condition ($p_o/p_a = 1.3$) is larger than that at the supersonic condition ($p_o/p_a = 2.5$). While for the case of jets from triangular and elliptic nozzles the growth of the jet at the supersonic condition is larger than that at the subsonic condition. The reason, as given above, can be explained as follows: Mixing between a supersonic jet and its surroundings occurs in two stages, an initial stage of bringing relatively large amounts of the fluids together (large-scale stirring). And a second stage promoted by the small-scale velocity fluctuations, which accelerate mixing at the molecular level, Panda [20]. Especially important is the rate at which fluid from the jet and from its surroundings become entangled or mixed as they join at the mixing layers. This information is given by the entrainment rate of the jet, which defines the rate of propagation of the interface between rotational and irrotational fluid, controlled by the speed at which the interface contortions with the largest scales move into the surrounding fluid. These controlling large-scale vortices tend to be coherent and easily recognizable features.

The growth of the twin jets in the x-y plane is shown in Fig.10-b. In the inner region, the width of the twin jet decreases due to the

streaming effect of surrounding entrainment and deflection of the axes of the twin jet. Far downstream from the nozzle exit plane the growth of the twin jet is greater compared to that of the single jet, Fig.10-a. This indicates that the combined jet spread more than the single jet, giving good mixing. The growth rate of the twin jet issuing from elliptic nozzles is greater than that of the triangular and circular jets.

The spread of the triple jet in the x-y plane is given in Fig.10-c. The spread rate of triple jets is negligible up to a distance of $x/d_e < 10$ after which the spreading closely follows that for the single jet. The spread rate of the triple elliptic jet increases by about 31% than that of the triple circular jet, for $p_o/p_a = 2.5$. This value for the triple triangular jet at the same initial conditions is 11%, indicating the large amount of entrainment created by elliptic jets. For the single jet, the corresponding values are 54% and 42%, respectively. This result indicates that the multiple jets spread with higher rate than the single jet. The present results are in good agreement with the previous data of Krothapalli, et. al. [13]. The difference between the spreading rates is attributed to the streaming effect of the entrainment fluid.

3.5 Flow visualization

The oil film visualizing method is a very useful technique to describe the complex flow field. Thus, the flow patterns of twin and triple jets have been filmed and compared with those of the single jet. Figure 11 shows the flow patterns of circular, triangular and elliptic jets. The spreading and decay of such jets are shown clearly. For twin and triple jets, in the region of jet convergence just downstream of the nozzle exit plane, the structure of the flow in the core of either jet is quite similar to that of a single free jet. Also, seen is the merging location at which the jets meet and the axial mean flow have positive direction downstream of the merging point, and negative direction upstream of the merging point. The fluid at the merging point is stagnant. Flow patterns of these jets suggest that the shear-layer disturbances are vortex rings and such vortices change with the nozzles geometry. It is seen also that the process of jet interaction has not depending on the nozzles geometry. While the spreading and decay rates are significantly affected by the nozzles geometry. Such results give good supporting to the measured data.

4. Conclusions

The interaction and mixing characteristics of twin and triple jets from triangular and elliptic nozzles are studied in comparison to those of axisymmetric jets, for subsonic ($p_o/p_a = 1.3$) and supersonic ($p_o/p_a = 2.5$) flow regimes. A study on the single jet is also made for comparison with multiple jets. In general, for all cases, the flow field of the single jet is characterized by the presence of three distinct regions as for the case of incompressible jets. These regions are the potential core region, a two-dimensional type region or the transient region depending upon the nozzles geometry and an axisymmetric type region. The single jet spreads linearly in the downstream direction and there is an empirical formula that governs the spreading of such jets. For the case of twin and triple jets, three distinct regions define the flow field: converging, merging and combined regions. In the converging region, the structure of the flow in the core of each jet is quit similar to that of a single jet. Compared to the circular jet, the triangular and elliptic jets spread only slightly faster at subsonic conditions, while at supersonic conditions, when screech occurs, they spread much faster. Screech profoundly increases the spreading of all jets. The screech effect changes for various nozzles geometry and the corresponding characteristics of flow field (spreading and decay rates) show enhanced entrainment and mixing properties relative to those of comparable axisymmetric jets. The phenomenon of axis switching is the main reason for enhancing the ambient entrainment. In fact, the present study of multiple non-circular jets provides some basic understanding of the mutual interaction of multiple jets and further application to the flame structure of gas burners, because the flame structure is affected by the mutual interaction of multiple jets.

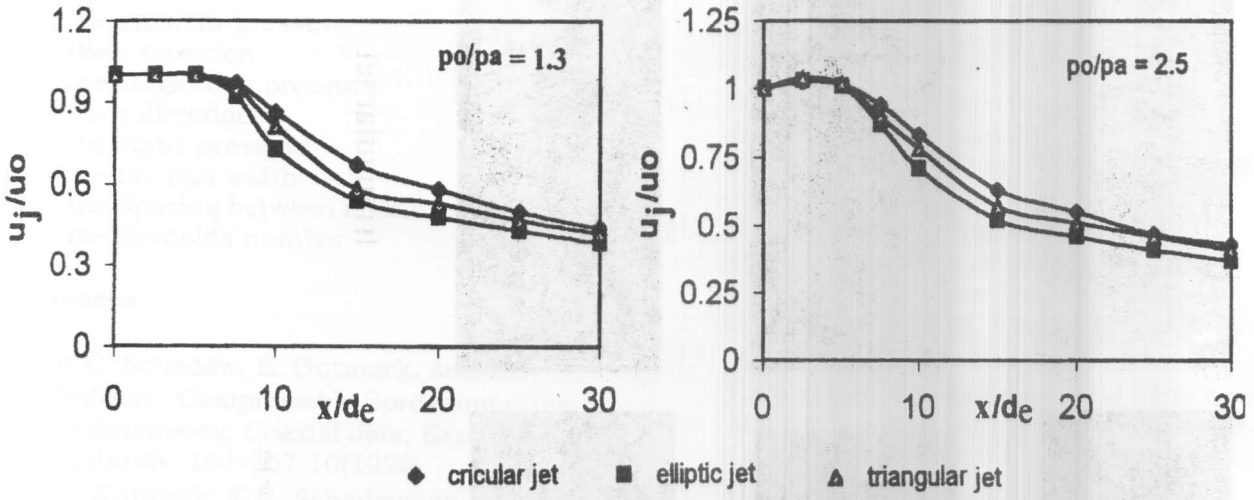

Fig. 9. Decay of axial mean velocity for triple jet.

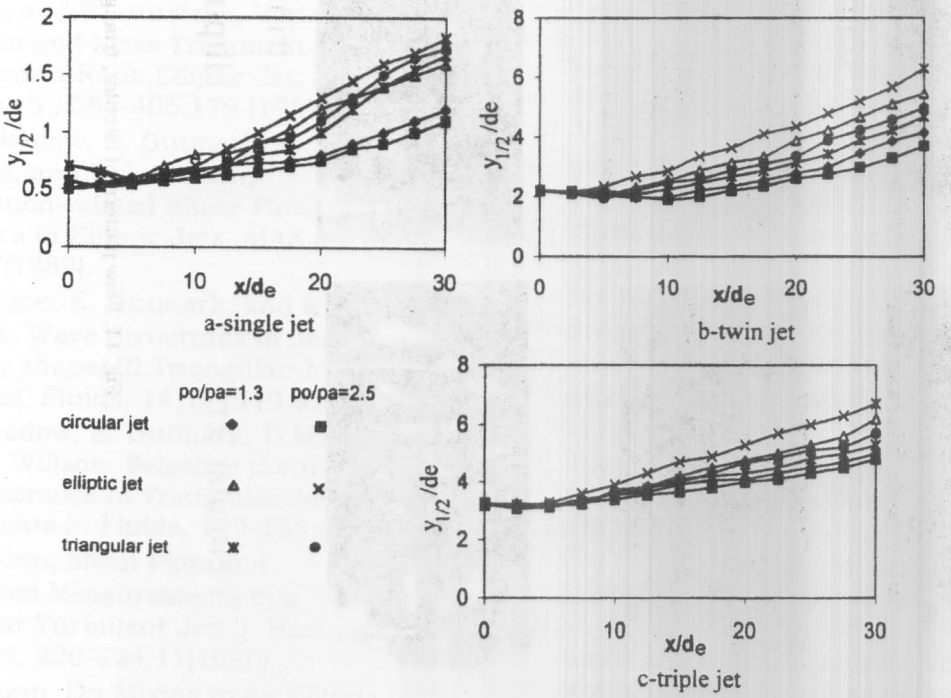

Fig. 10. Growth of the half width of single jet.

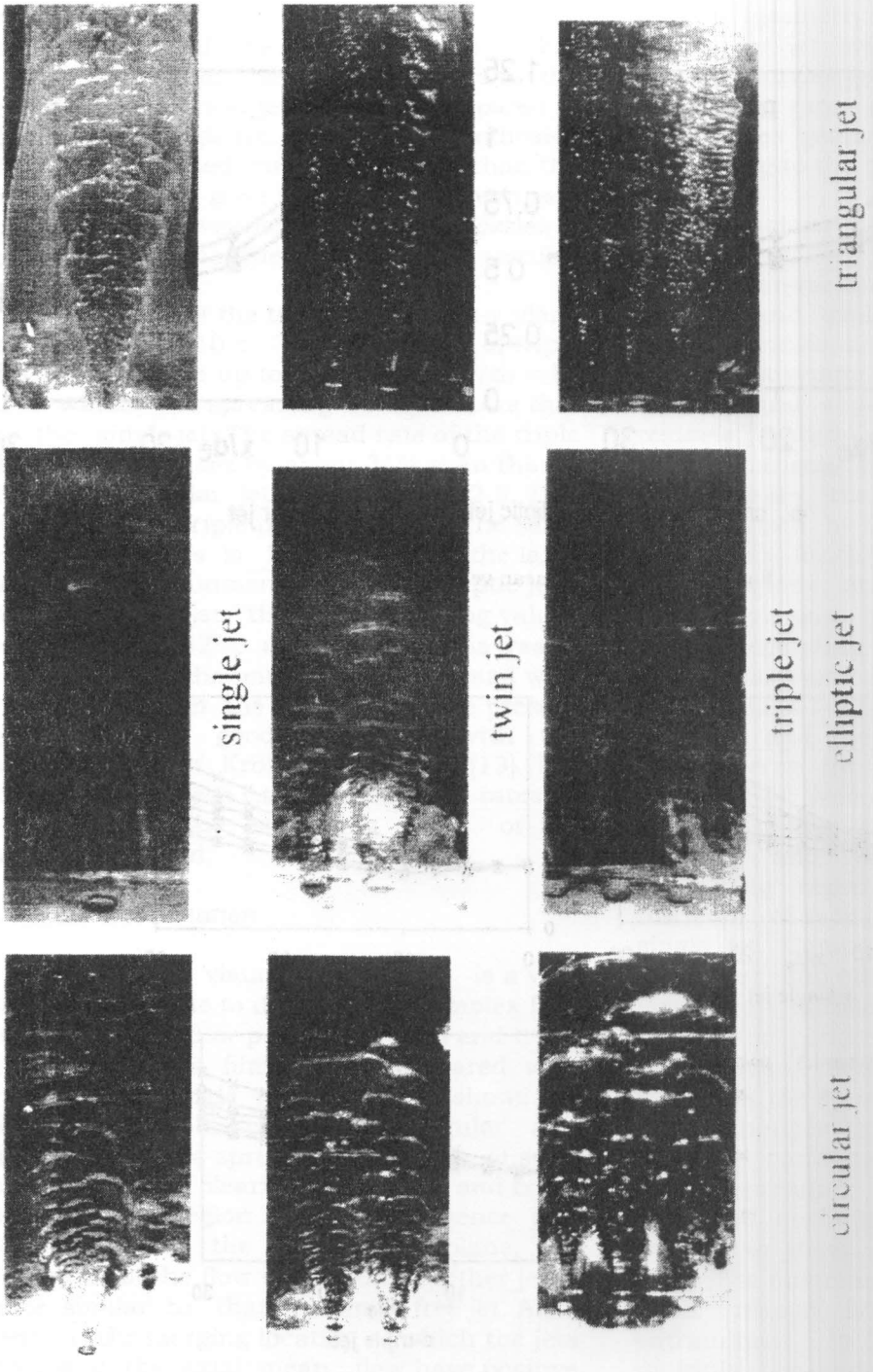

Fig. 11. Flow pattern of circular, triangular and elliptic jet.

Nomenclature

a is the ambient condition
u_j is the velocity for each jet
d_e is the nozzle exit diameter
u_o is the velocity at nozzle exit
D_e is the equivalent diameter
u_{ax} is the velocity at symmetric axis

M_e is the Mach number at nozzle exit
x is the x direction
p_a is the ambient pressure
y is the y direction
P_o is the stagnation pressure
z is the z direction
P_s is the static pressure
$y_{0.5}$ is the the half width
S is the Spacing between nozzle axes
Re is the Reynolds number

References

[1] K.C. Schadow, E. Gutmark, and K.J. Willson, Compressible Spreading rates of Supersonic Coaxial Jets, Experiments in Fluids, 161-167,10(1990).

[2] E. Gutmark, K.C. Schadow, and K.J. Willson, Effect of Convective Mach Number on Mixing of Coaxial Circular and Rectangular jets, Physics of Fluids, 29-35,3(1991).

[3] C.M.Ho, and E. Gutmark, Vortex Induction and Mass Trainment in a Small Aspect Ratio Elliptic Jet, J. of Fluid Mech., 383-405,179 (1987).

[4] K.C. Schadow, E. Gutmark, S. Koshigoe, and K.J. Willson, Combustion-related Shear Flow Dynamics in Elliptic Jets, AIAA J., 1347-1353,27(1989).

[5] S. Koshigoe, E. Gutmark, and K.C. Schadow, Wave Structures in Jets of Arbitrary shape, III Triangular Jets, Physics of Fluids, 1410-1419,31 (1988).

[6] K.C.Schadow, E. Gutmark, D.M. Parr, and K.J. Willson, Selective Control of Flow Coherence in Triangular Jets, Experiments in Fluids, 129-135,6(1988).

[7] W.R. Quinn, Mean Flow and Turbulence Measurements in a Triangular Turbulent Jet, J. Heat and Fluid flow, 220-224,11(1990).

[8] W.R. Quinn, On Mixing in an Elliptic Turbulent Free Jet, Physics of Fluids, 1716-1722,A1(10) (1989).

[9] E. Gutmark, and F.E. Grinstein, Flow Control with Noncircular Jets, Annu. Rev. Fluid Mech., 239-272, 31 (1999).

[10] T. Okamoto, M. Yagita, A. Watanabe, and K. Kawamura, Interaction of Twin Turbulent Circular Jet, Bul. of JSME, 617-622, 28(1985).

[11] E. Tanaka, The Interference of Two Dimensional Parallel Jets (1st Rept., Experiments on Dual Jet), Bul. of JSME, 272-280, 13 (1970).

[12] E. Tanaka, The Interference of Two Dimensional Parallel Jets, (2nd Rept. Experiments on the Combined of Dual Jet), Bul. of JSME, 920-926, 17 (1974).

[13] A. Krothapalli, D. Baganoff, and K. Karamcheti, Development and Structure of a Rectangular jet in a Multiple Jet Configuration, AIAA J, 945-950, 15 (1980).

[14] E. Tanaka, and S. Nakata, The Interference of Two Dimensional Parallel Jets, (3rd Rept. The Region Near the Nozzles in Triple Jets), Bul. of JSME, 1134-1141, 18 (1975).

[15] D.R. Miller, and E.W Comings, Force Momentum Fields in Dual Jet Flow, J. of Fluid Mechanics, 237-256, 7(1960).

[16] Y.F. Lin, and M.J.Sheu, Interaction of parallel Turbulent Plane Jets, AIAA J., 1372-1373, 29(1991).

[17] S. Koshigoe, E. Gutmark, and K.C. Schadow, Initial Development of Noncircular Jets Leading to Axis Switching, AIAA J., 411-419, 27(1989).

[18] S. Raghunathan, and I.M. Reid, A Study of Multiple Jets, AIAA J., 124-127, 19(1981).

[19] Namer and V. Otugen, Velocity Measurements in a Plane Turbulent Air Jet at Moderate Reynolds Numbers, Experiments in Fluids, 387-399,6 (1988).

[20] J. Panda, Shock Oscillation in underexpanded Screeching Jets, J. Fluid Mech., 173-198, 363(1998).

[21] A.H. Shapiro, The dynamic and thermodynamics of compressible fluid flow, Ronald press, New York (1953).

Received January 27. 2000
Accepted July 6, 2000